Project Number: [956004]
Project Acronym: [BioTrib]
Project title: [Advanced Research Training for the Biotribology of Natural and Artificial Joints in the 21st Century]

BioTrib Deliverables Report – Niccoló De Berardinis

Deliverable: D3.5 *In vitro data on cell biocompatibility and antibacterial properties*

Month Due: PM36
Month Delivered: PM36

Project coordinator name	Dr Gregory de Boer
Project coordinator organisation name	UNIVLEEDS
Report prepared by	Niccoló De Berardinis Gry Hulsart Billström Hanna Nilsson Åhman Cecilia Persson

Dissemination Level of Report

PU	Public	x
PP	Restricted to other program participants (including the Commission Services)	
RE	Restricted to a group specified by the consortium (including the Commission Services)	
CO	Confidential, only for members of the consortium (including the Commission Services)	

The BioTrib ETN project has received funding from the European Union's Horizon 2020 research and innovation programme under grant agreement No. 956004.

Version	Date	Comment	Modifications made by
D**3.5.1**	20-12-2023	First Draft circulated to Richard M Hall, Gregory de Boer, Judith Schneider, Gry Hulsart Billström and Cecilia Persson	Richard M Hall
D3.5.2	28-12-2023	Review and Amendment	**Niccoló De Berardinis, Gry Hulsart Billström**
D3.5.3	29-12-2023	Second Draft circulated to Richard M Hall, Gregory de Boer, Judith Schneider, Gry Hulsart Billström and Cecilia Persson	
D3.5.4	29-12-2023	Circulated to the Scientists in Charge with minor amendments.	Richard M Hall
D3.5.5	08-01-2024	Review and Amendment	**Niccoló De Berardinis, Gry Hulsart Billström, Cecilia Persson**
D3.5.6	10-01-2024	Third Draft circulated to Richard M Hall, Gregory de Boer, Judith Schneider, Gry Hulsart Billström and Cecilia Persson	**Niccoló De Berardinis, Gry Hulsart Billström, Cecilia Persson**
D3.5.7	31-01-2024	Sign-off at Supervisory Board	-
D3.5	**01-02-2024**	**Submitted to Commission**	**Judith Schneider (UNIVLEEDS)**

Contents

Executive Summary – PBF-LB processed WE43 exhibits high levels of cytocompatibility.

Novel biodegradable implants are required in the orthopaedic field to reduce implant-removal surgery costs and limit patient stress and related risks (e.g., anesthesia, recovery time). The focus in this field has fallen on magnesium-based alloys as the material of choice for producing third-generation biomaterials for bone implants due to their biodegradability, good mechanical properties, and good biocompatibility. Traditional manufacturing methods for these alloys (casting and extrusion) are already used today for the production of magnesium alloys used in the clinic with European certification, such as WE43 (4 wt% Y, 0.5 wt% Zr, rare-earths ~3 wt%). These methods have limitations in achieving intricate designs and the potential design freedom that an additive manufacturing process might offer. These could offer a wide variety of mechanical and biological improvements, for example, creating a bone-like trabecular structure to improve cell proliferation and osteointegration or improving the material properties by enhancing its design. The PBF-LB additive manufacturing of Mg-alloys, although promising for creating such samples with intricate and optimized designs, for now struggles with achieving acceptable corrosion resistance comparable to its extruded counterparts, and further improvements are still necessary. The study biologically evaluates the use of the powder bed fusion laser beam technique (PBF-LB) for the 3D-printing of the WE43 Mg-alloy (3D-WE43) by assessing the cytocompatibility of 3D-WE43 in comparison with established materials well-used in the clinic, such as extruded Ti64 and extruded WE43. This evaluation involves in vitro cytocompatibility studies using the MC3T3-E1 cell line and antibacterial testing against E. coli. The results indicate that 3D-WE43 exhibits high levels of cell proliferation (110%) and cytocompatibility, matching or exceeding that of the extruded counterpart (80%) or the untreated control group (100%). Furthermore, although the antibacterial study revealed limited efficacy in preventing the growth of E. coli, this was also the case for materials such as Ti64, which are the current state of the art alloy for orthopaedic surgeries. The overall cytocompatibility makes 3D-WE43 a promising material for producing biodegradable implants. This work highlights the potential of PBF-LB processed WE43 to produce biodegradable implants. Despite its current challenges in corrosion resistance, its high cytocompatibility makes 3D-WE43 a valuable candidate for exploring its innovative orthopedic applications.

Introduction

PBF-LB (Powder Bed Fusion Laser Beam) is an advanced additive manufacturing method that enables the production of Mg-based samples with intricate designs [1]. The PBF-LB printing of the Mg alloy WE43 (4 wt% Y, 3 wt% rare-earth elements) has shown great potential for the development of biodegradable implants in the orthopaedic field [2], but despite its promise, it has some challenges due to reactivity of the material [3]. The 3D-printed WE43 (3D-WE43) has yet to achieve acceptable corrosion resistance, at least equal to that of its extruded counterpart, while maintaining adequate mechanical properties. In addition, corrosion during the degradation of magnesium can affect biocompatibility [4]. Therefore, we aimed to evaluate the cytotoxicity of the material in comparison to established materials in the clinic (e.g., extruded Ti64 and extruded WE43). The antibacterial potential of the alloy was also assessed.

Material and Methods

a. Cytocompatibility study

The *in vitro* cytocompatibility was evaluated using the mouse-derived osteoblastic cell line MC3T3-E1 Subclone 4 (ATCC). Material extracts were evaluated according to ISO 10993- 5/12 in a 3-day end-point experiment. The results for the PBF-LB processed WE43 alloy (3D-WE43) were compared against four control groups, namely: untreated cells, extruded WE43 (extr-WE43), extruded Ti64 (extr-Ti64) grade 23 and medium containing 3% DMSO (Dimethyl sulfoxide) (toxic control). The experiment was repeated in three independent biological replicates with six technical replicates. To prepare the extracts, all samples were first sterilized by immersion in isopropanol (Sigma, 190764-1L) in combination with ultrasound for 5 minutes. The samples were then quickly rinsed in PBS (Gibco, 20012-019) and allowed to dry in a sterile environment. The samples were then immersed in cell media for 24 h in an incubator (37 °C, 95% humidified environment and 5% CO2) to produce conditioned media for each material to be tested. A ratio of material to cell medium of 125 mm^2/ml was used. A cell medium consisting of alpha-MEM (Cytiva, SH30265.01, Sweden) containing 10% FBS (Sigma, USA) and 1% pen-strep (Gibco, USA) was used.

One day prior to the start of the experiment 10 000 cells per well were seeded in a 96 well-plate and allowed to adhere and form a semi-confluent cell layer overnight. The following day, the medium was replaced with fresh media for the untreated control group and conditioned media for the other groups. In addition, a 3% DMSO plus medium solution was added as an extra control group as a toxic agent. The cells were then placed in an incubator for three days. The mitochondrial metabolism of cells exposed to the conditioned media for three days was then assessed with the AlamarBlue HS viability assay. This assay can be seen

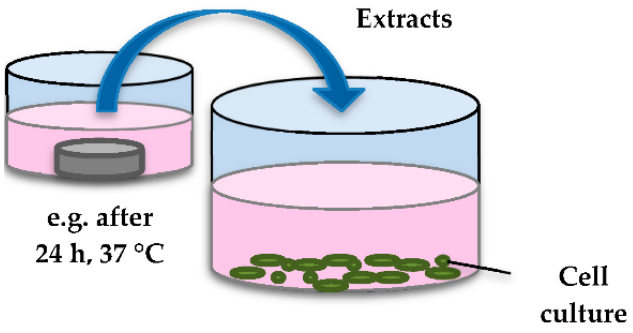

Figure 1. Scheme for the production of conditioned media from solid samples with known surface area (125 mm^2/ml) following the ISO standard 10993 part 5 & 12 recommendations. Amended figure from reference: E. Scarcello, D. Lison (2020). "Are Fe-Based Stenting Materials Biocompatible? A Critical Review of In Vitro and In Vivo Studies". J. Funct. Biomater. 2020, 11(1),2. https://doi.org/10.3390/jfb11010002. Creative Commons License 4.0 - CC BY 4.0 DEED

as a measure of their metabolic activity, and thus as an approximate measure of the total number of cells. The media with extracts was removed and replaced with a 10% Alamar Blue HS (Invitrogen, A50100) solution in the cell medium. The solution was left for 3 h in the incubator, after which the supernatant was moved into a black 96 well-plate and the fluorescence intensity was measured using an excitation wavelength of 560 nm (540-570 range) and emission wavelength of 590 nm (580-600 range). Another enzymatic activity assay

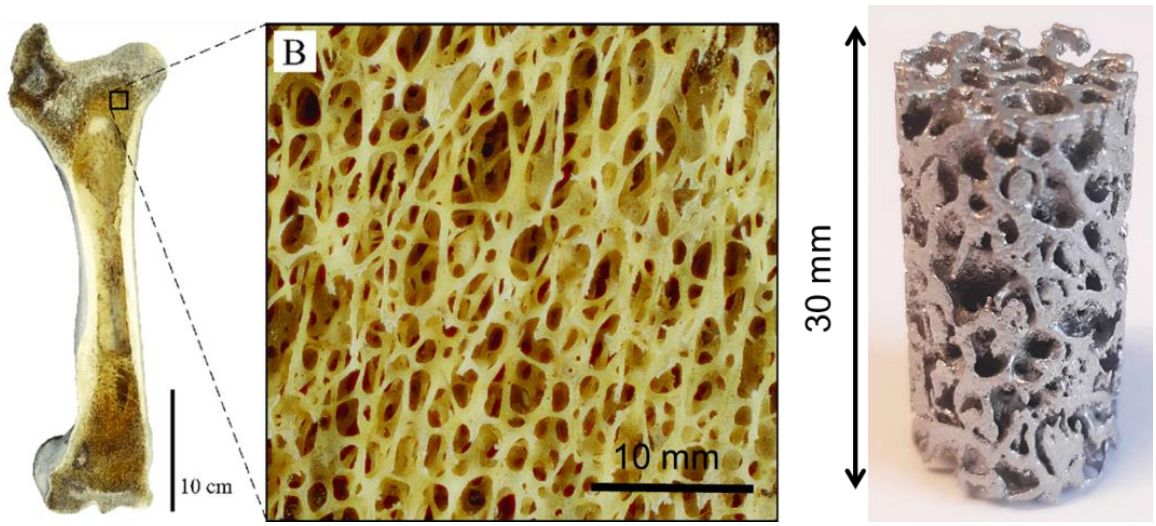

Figure 2. 3D-printed trabecular structure sample using the PBF-LB technique compared with natural trabecular bone tissue. Figure A & B amended from reference: Bishop P et al 2018. https://doi.org/10.7717/peerj.5778. Creative Commons License 4.0 - CC BY 4.0 DEED

was also performed on the same wells measuring the LDH (lactate dehydrogenase) activity of fully lysed cells after the initial AlamarBlue assay. To remove any dead cells or traces from previous assay, the cells were first briefly washed with PBS. RIPA lysis buffer (Thermo Scientific, 89901) was then added to each well. The plate was subsequently placed on a plate shaker for 15 min at 65 RPM in room temperature to allow uniform lysis of the cells throughout the plate. After complete lysis, part of the supernatant from each well was mixed (50:50) and left to react with an LDH substrate solution (Invitrogen, C20300) for 30 min at room temperature, protected from light. Thereafter, the absorbance was measured at 490

nm and 680 nm. The proliferation was calculated by comparing it to the initially 10 000 seeded cells. The final dataset consisted of three independently repeated assays for each of the six technical replicates used for each group for both cellular assays. The three repeated assays were normalized to the corresponding untreated control group and set as the maximum percentage (100%).

b. Statistical analysis

Statistical analysis in the form of a one-way ANOVA test and a post hoc Tukey's test was performed in GraphPad Prism (Version 6.01) to assess any statistical difference (taken at $p < 0.05$) between the controls for both cellular assays.

c. Antibacterial properties study

To determine the antibacterial properties of 3D-WE43, a 24 h end-point zone of inhibition experiment was performed on E. coli. A 0.5 McFarland standard was prepared, whose density is comparable to 1.5 x 10^8 CFU/ml, and nine separate Petri dishes were prepared with that concentration of cells growing on agar. Three samples of Ti64, ex-WE43 and 3D-WE43 were placed in the middle of one dish each, and the cells were incubated with the materials for 24 h at 37 °C. After that, pictures of each dish were taken.

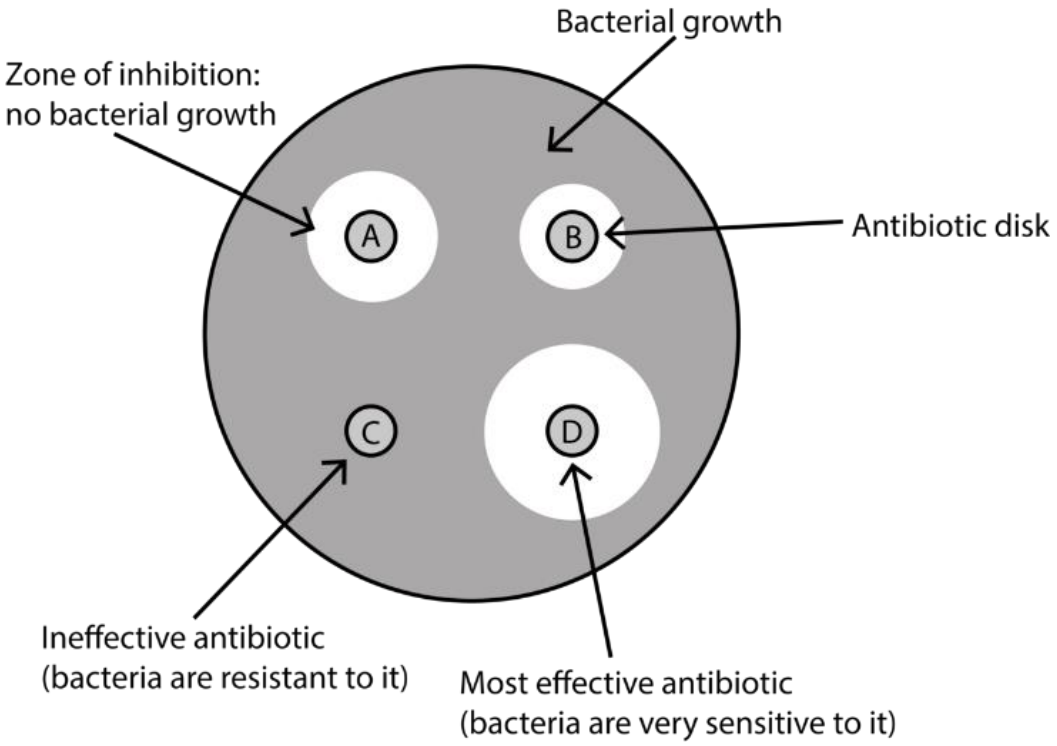

Figure 3. Diagram of an inhibition zone experiment showing the effectiveness of the antibiotic against bacterial colony growth. Images reference: https://commons.wikimedia.org/wiki/File:Zones_of_Inhibition.png

Results and discussion

All groups (figure 1), apart from Extr-WE43, showed fully biocompatible cell proliferation levels measured by LDH activity, with an average proliferation of 100% or more compared to

the untreated cells. Here, 3D-WE43 showed the highest value (110%). While there was no statistically significant difference in proliferation score between 3D-WE43 nor Extr-WE43 compared to the control and the extruded Ti64 group, 3D-WE43 showed a significantly higher proliferation ($p < 0.01$) than Extr-WE43. While the Extr-WE43 gave the lowest proliferation (80% compared to the control group), it was still in the non-toxic range (>70%). The toxic agent group (DMSO) showed a decrease in cell proliferation and growth (32% compared to the untreated cells), consistent with the toxic effect of DMSO previously reported in the literature [5] [6] [7]. For the resazurin reduction dataset in Figure 1, all groups showed similar cytocompatible behavior with no statistical differences in each of the groups and when compared to the untreated group, further confirming the biocompatibility of all biomaterials considered in this study. The present viability tests indicate that the PBF-LB processed WE43 has the potential for future application as a biodegradable metal implant. As the degradation rates of the bulk get lower, further research into biocompatibility by direct cell seeding and *in vivo* tests should be explored.

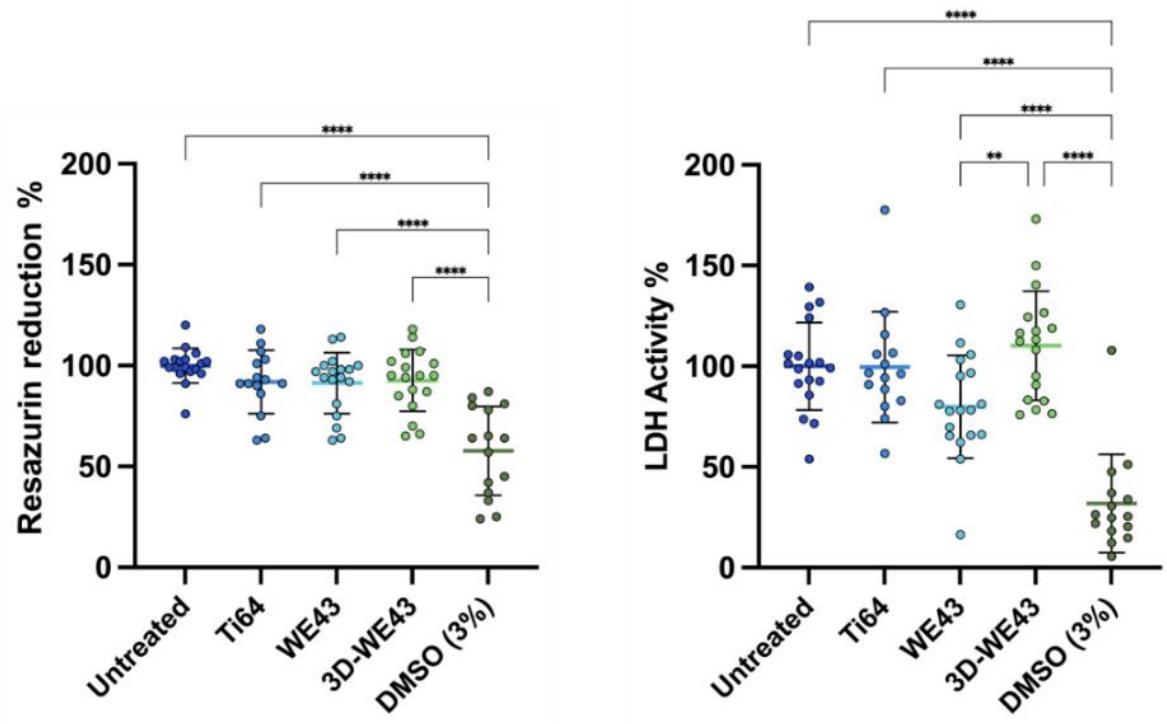

Figure 4. Resazurin reduction and LDH activity percentage, measured by Alamar Blue and LDH cytotoxicity assay, of a three-day end-point experiment with MC3T3-E1 pre-osteoblasts cultivated with and without conditioned media produced from different materials (i.e., titanium 64, extruded WE43 and #d-printed WE43) and a toxic control group (3% DMSO). A one-way ANOVA statistical test with Tukey *post hoc* correction was performed for all of the datasets (* $p < 0.05$; ** $p < 0.01$; *** $p < 0.001$; **** $p < 0.0001$).

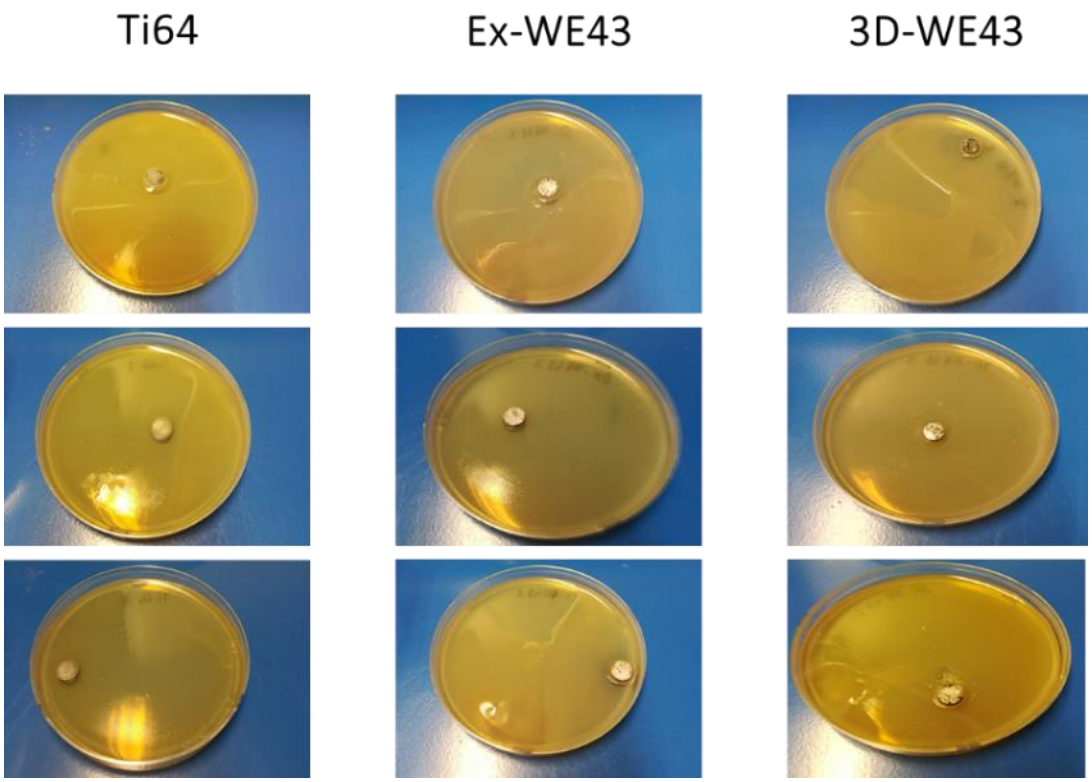

Figure 5. Zone of inhibition antibacterial testing of different biomaterial (from left to right: titanium 64, extruded WE43 and 3D-printed WE43) cultured with E. coli for 24 h at 37 °C.

As shown in Figure 2, all biomaterials appear to lack a strong antibacterial effect on E. coli since a clear zone of inhibition ring was not present around the samples. This appears consistent to what has been found in the literature, meaning WE43 alloy, both extruded and 3D printed, seems to not have an pronounced antibacterial effect on E. coli [8]. Also, even if Ti64 is commonly used as a material for bone implants, this titanium alloy is biologically inert and does lack of antibacterial properties [9]. Therefore, in order to achieve an antibacterial effect using WE43-based Mg alloy, it is necessary to either modify the surface [10] or the material composition [8] by adding some antibacterial elements, such as copper or zinc. However, in our samples, a slightly lighter area was present around some samples. The diameter of these areas is shown in table 2. From these measures, it appears that Ti64 has the largest light areas compared to the other biomaterials, but bacterial cells were still present around it.

Table 1. Diameter in mm of the lighter-looking areas around the different Ti64, ex-WE43 and 3D-WE43 samples after 24 h in incubation with E. coli in an antibacterial zone inhibition test and samples diameters.

	Ti64	Ex-WE43	3D-WE43
Diameter (mm)	14.3 ± 2.1	15.0 ± 1.4	12.0 ± 2.8
Samples Diameter (mm)	9	8	8.5
Diameter - Sample (mm)	5.3	7	3.5

Conclusion

The present cytocompatibility and antibacterial tests indicate that the PBF-LB processed WE43 has the potential for future application as a biodegradable metal implant. This warrants further *in vitro* investigations, such as cell differentiation, RNA expression, collagen, and mineralised extracellular matrix production, to achieve an enhanced understanding of the material's osseointegration properties. Furthermore, it is recommended to deepen the research using a more refined and sensitive antibacterial test than the current one. This approach is essential to ascertain whether there are subtle variations in the antibacterial properties of the chosen materials. This will provide a more complete view of the effectiveness and possible applications of these materials in contexts where antibacterial properties are crucial.

References

[1] W. Wang and Y. Xia, “Topology optimization based channel design for powder-bed additive manufacturing,” *Addit. Manuf.*, vol. 54, p. 102717, Jun. 2022, doi: 10.1016/j.addma.2022.102717.

[2] H. Nilsson Åhman, L. Thorsson, P. Mellin, G. Lindwall, and C. Persson, “An Enhanced Understanding of the Powder Bed Fusion–Laser Beam Processing of Mg-Y3.9wt%-Nd3wt%-Zr0.5wt% (WE43) Alloy through Thermodynamic Modeling and Experimental Characterization,” *Materials*, vol. 15, no. 2, p. 417, Jan. 2022, doi: 10.3390/ma15020417.

[3] J. Liu *et al.*, “Improving corrosion resistance of additively manufactured WE43 magnesium alloy by high temperature oxidation for biodegradable applications,” *J. Magnes. Alloys*, p. S2213956722001992, Sep. 2022, doi: 10.1016/j.jma.2022.08.009.

[4] J. Kim and H. Pan, “Effects of magnesium alloy corrosion on biological response – Perspectives of metal-cell interaction,” *Prog. Mater. Sci.*, vol. 133, p. 101039, Mar. 2023, doi: 10.1016/j.pmatsci.2022.101039.

[5] P. V. Dludla *et al.*, “A dose-dependent effect of dimethyl sulfoxide on lipid content, cell viability and oxidative stress in 3T3-L1 adipocytes,” *Toxicol. Rep.*, vol. 5, pp. 1014–1020, 2018, doi: 10.1016/j.toxrep.2018.10.002.

[6] N. F. Sangweni, P. V. Dludla, N. Chellan, L. Mabasa, J. R. Sharma, and R. Johnson, “The Implication of Low Dose Dimethyl Sulfoxide on Mitochondrial Function and Oxidative Damage in Cultured Cardiac and Cancer Cells,” *Molecules*, vol. 26, no. 23, p. 7305, Dec. 2021, doi: 10.3390/molecules26237305.

[7] H. Lee and J.-B. Park, “Dimethyl Sulfoxide Leads to Decreased Osteogenic Differentiation of Stem Cells Derived from Gingiva via Runx2 and Collagen I Expression,” *Eur. J. Dent.*, vol. 13, no. 02, pp. 131–136, May 2019, doi: 10.1055/s-0039-1694904.

[8] O. Esmaielzadeh, A. R. Eivani, M. Mehdizade, S. M. A. Boutorabi, and S. M. Masoudpanah, “Investigation of mechanical properties and antibacterial behavior of WE43 magnesium-based nanocomposite,” *Mater. Chem. Phys.*, vol. 293, p. 126864, Jan. 2023, doi: 10.1016/j.matchemphys.2022.126864.

[9] G. Yang, H. Liu, A. Li, T. Liu, Q. Lu, and F. He, “Antibacterial Structure Design of Porous Ti6Al4V by 3D Printing and Anodic Oxidation,” *Materials*, vol. 16, no. 15, p. 5206, Jul. 2023, doi: 10.3390/ma16155206.

[10] V. K. Manivasagam *et al.*, "Surface-modified WE43 magnesium alloys for reduced degradation and superior biocompatibility," *Vitro Models*, vol. 1, no. 3, pp. 273–288, Jun. 2022, doi: 10.1007/s44164-022-00016-x.